International Journal on Electrical Engineering and Informatics - Volume 13, Number 4, December 2021

Performance Enhancement of PV Grid Connected Systems with Different Fault Conditions

Saad A. Mohamed Abdelwahab[1, 3], Adel A. Elbaset[2,4], Fahd Yousef [1], Walid S.E. Abdellatif [1,5]

[1]Electrical Department, Faculty of Technology and Education, Suez University, Suez, Egypt.
[2]Electrical Engineering Department, Minia University, El-Minia, 61517, Egypt.
[3]High Institute of Electronic Engineering, Ministry of Higher Education, Bilbis- Sharqiya, Egypt.
[4]Department of Electromechanics Engineering, Faculty of Engineering, Heliopolis University, Cairo, Egypt.
[5]Department of Electronics and Electrical Communications Engineering, Higher Institute of Engineering and Technology, Ministry of Higher Education – Kafr Elsheikh, Egypt.
saad.abdelwahab@suezuniv.edu.eg, Adel.Soliman@mu.edu.eg, fahdyousef12345@gmail.com, walid.abdellatif@suezuniv.edu.eg

Abstract: PV energy is abundant and sustainable energy that photovoltaic (PV) cells can transform directly into electricity. The PV array output energy is dependent on the change in solar radiation and temperature**.** Maximum Power Point Tracking (MPPT) techniques are used in the PV systems to track maximum energy under rapidly changing weather conditions. Also, the rapid increase of Solar energy penetration in the electric grid necessitates keeping connected to the grid during abnormal operating conditions, especially voltage sag and grid short circuit. This paper presents the modeling and simulation of MPPT of a grid-connected PV system with the incremental conductance (INC) technique. INC results compared with perturbing and observe (P&O) scheme. Also, to analyze the PV system during faults on utility power grid and determine the effects of faults as a function of the location where the fault occurs. Improving the fault ride-through (FRT) capability of PV system during faults on the utility power grid by s Crowbar Strategy is introduced in this paper. The performance is estimated and compared by mathematical investigation and simulation analysis. To validate the correctness of the proposed methods is used the MATLAB /Simulink toolbox. The performance of the proposed INC MPPT indicates that the INC reaches the optimum power point more effectively than the (P&O) scheme, in addition; the FRT capability enhancement by using the crowbar technique. This article introduces the MPPT of a grid-connected PV system as a simulation and experimentally tracks the speed of PV radiation change in different operating conditions.

Keywords: Maximum power point tracking, fault ride-through, incremental conductance, and crowbar.

1. Introduction

A new approach to using renewable energy due to growing concern about environmental issues is increasing fuel prices. The conversion efficiency is very low for solar power systems, especially under the changing conditions of the ever-changing solar radiation. Recently it has been noted that the system connected to the network Photoelectric has become more advanced. There must be fairly large areas to produce much of this electrical energy to meet this increasing demand for electrical energy. Therefore, new maximum energy extraction techniques must be used to track the power point of these arrays [1-5].

Many papers are classified as a development of the PV system with MPPT methods in the last few years. The MPPT of direct methods to find MPP such as perturb and observe (P&O) [6-11], incremental conductance (INC) technique [12-13], sliding mode control, fuzzy logic control [14-18] and Current sweep and Constant voltage and Temperature Method and Fixed duty cycle and MPP Locus Characterization and Beta Method and System Oscillation and Ripple Correlation. There are many methods for MPPT, but in this paper, we will cover only two

Received: September 24th, 2021. Accepted: December 2th, 2021
DOI: 10.15676/ijeei.2021.13.4.8

methods, INC & P&O. The second problem for grid-connected solar systems is the sudden drop in grid voltage. Low Voltage Ride Through Technology (LVRT), as a powerful power grid fault recovery support, is attracting more and more attention. The general LVRT requirements of PV generation systems focus on keeping transformers in contact with the electrical network in short periods of low electrical grid voltage. Many methods have been used in previous research to improve LVRT. However, these methods had some limitations. Fault removal and fault location are concentrated in [19], showing fault clearance, and fault location and emphasis are given to network connectivity in the current source inverter in [20]. Still, both papers did not consider MPPT during the fault. In [21] it has been proposed to prevent voltage degradation due to fault in the network side. An expensive superconducting fault current limiter for use with photovoltaic systems, it also uses partial open-circuit voltages [19-23]. All the previously mentioned cases do not work except in the case of constant solar radiation and do not work with solar radiation that changes with time. Despite this, the computer graph and its severity can start to go wrong. An event caused by a current caused by a superconducting current.

This paper proposes an efficient and usable control system based on the INC and P&O methods to achieve the MPPT from PV system under different conditions. INC and P&O are studied under various conditions of differing temperature, solar irradiance values. The main contribution of this paper is the practical and mathematical investigation of the proposed method. Besides, to analyze the PV system during faults on utility power grid and determine the effects of faults as a function of the location where the fault occurs. Improving the fault ride-through (FRT) capability of PV system during faults on the utility power grid by s Crowbar Strategy presents the research in the following organization, system description, MPPT techniques, voltage ride-through, simulation results, and discussion, experimental work, and finally, the conclusions.

2. System Description

The general system of the Grid-connected PV system is shown in Fig.1, its one of two stages of solar power systems connected to the grid. Stage number one contains a DC-DC converter. This makes better use of the PV array by greatly reducing the shading effect for the entire system. Stage number two contains three-phase VSC DCAC inverter.

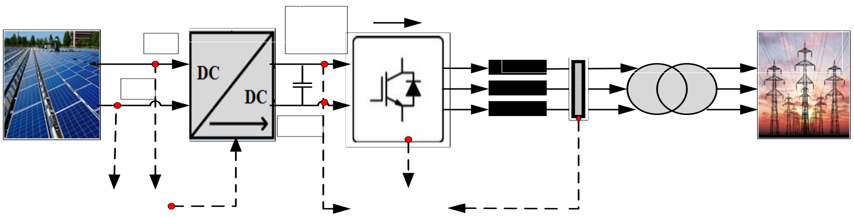

Figure 1. The proposed system of the grid-connected PV array.

The conventional control system for the Grid-connected PV system consists of two stages into two main parts, the boost converter control and the inverter control. The first part is the boost converter composed of an Insulated-Gate Bipolar Transistor switch (IGBT), inductor, diode, and capacitor. The 5 kHz booster converter increases the normal DC voltage of the cell from 273 to 500 V (MPPT) is implemented in the dc-dc boost converter employing a State flow implementation using one of the (MPPT) techniques To generate the voltage required to extract the maximum power, this type of MPPT controller automatically changes the switching duty cycle. The three-phase VSC Dc Ac reflector control unit is the second part and consists of a switching unit that contains a closed-phase loop (PLL) phase and a DQ coordinate transformation. It also consists of a power balance controller with a PI voltage feedback controller DC link and proportional-integral (PI) regulators. The 2000-Hz DC-AC inverter VSC converts the dc-link voltage from 500Vdc to 260Vac and keeps unity power factor. The model also includes an appropriate inductance filter to remove the high order harmonics from the voltage and the current of the inverter. The PV array uses 330 SunPower SPR-305-WHT modules (165 strings of 5 series-connected modules connected in parallel) [11]. The inputs of PV Array are the sun irradiance (W/m2) and the cell temperature (°C).

A. PV Array Modelling

Figure 2 displays the parabolic circuit model of a PV cell. Series–parallel combination of PV cells forms a PV array with a specified rating of current and voltage [1].

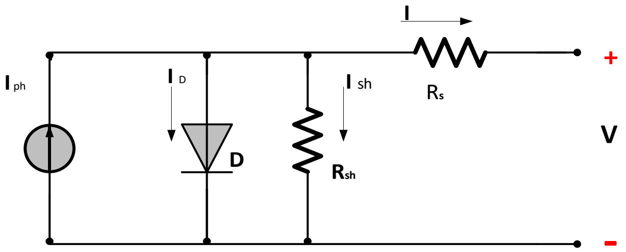

Figure 2. PV cell parabolic circuit [17].

In the equation below, namely "the central equation depicting V-I curves for photoelectric cells", the production stream is defined by [1].

$$\mathbf{I} = \mathbf{I_{Ph}} - \mathbf{I_0}\left[\mathbf{e}^{\frac{\mathbf{q(V+IR_S)}}{\mathbf{AKT_C}}} - \mathbf{1}\right] - \frac{\mathbf{V + IR_s}}{\mathbf{R_{Sh}}} \tag{1}$$

Where: I is the PV current of the PV module, the saturation current of the diode is I_0, I_{Ph} is the -generated current from photo, R_S is the resistance of series in Ω, R_{Sh} is the resistance of parallel in Ω, n is the ideality factor, the constant of Boltzmann is K, the charge of electron is q and T is the temperature [°K].

B. DC-DC Boost Converter

This circuit is used to increase the PV output voltage. The DC/DC boost converter is concerned with investigating the required and synchronized voltage level and with the electrical grid by DC/AC inverter as shown in Fig. 3. Fig. 3, displays the configuration of a boost DC-DC converter that contains an electricity coil; L with an inner resistance of R, a diode; D; and a DC-link-capacitor; C and (IGBT) switch. The detailed model increases the voltage from 280V to 500V by the boost converter. The boost converter makes use of MPPT technique that's straight-up changes the duty cycle to generate the desired voltage to produce maximum energy from the PV array. The key to tracking process in most MPPT technologies is changing of booster duty cycle *D*s the modulation index of the boost converter control maintains changing so that voltage output can track the desired voltage under variable solar radiation [6]

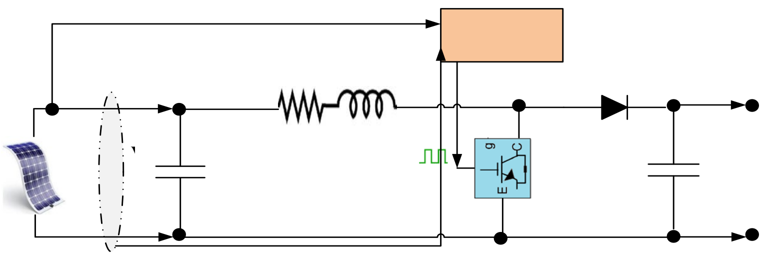
Figure 3. the illustrative circuit of DC-DC boost converter.

Stepping-up, its magnitude of input voltage to a value desired employing electronic switching, is the main purpose of the DC-DC booster circuit. However, the output voltage from the PV array has a small value to be synchronized with the electrical grid through the DC/AC inverter. Therefore, the DC/DC boost converter works to step up the PV output voltage and achieve the desired voltage equal (500 V). The output of the boost converter is specified to the three-phase inverter. The MPPT controller gives PWM pulses to IGBT [17-19] to keep the output voltage constant.

3. MPPT Techniques

PV cell V-I quality isn't linear and differs with heat and irradiation. Generally, a distinctive point on the V-I or V-P curve is named the Maximum Power Point (MPP). The whole PV system (array, converter, etc…) operates with maximum qualification and makes its maximum output energy. The rhythmic of the MPP is unbeknown but can be existed. It can be done by calculating models or by searching algorithms. So, the maximum Power Point Tracking (MPPT) strategy needs to maintain the PV array's operating point at its MPP. But in this thesis my method will be implemented the (P&O) methods and the (IC) methods.

A. Incremental Conductance method (INC)

The INC method is built on the power-voltage ramp as exposed in Fig.4. The INC MPPT flow chart, as exposed in Fig.5, the slope of the P-V properties calculated, it is positive if the action point on the left side of the MPPT, therefore it is stimulated to the truth by increasing the PV voltage. But if the slope of the typical curve is negative, the procedure assumes that the point of operating exists on the side of the MPP right, and therefore it must be encouraged to the left by reducing the PV cells voltage [1].

The IC MPPT flow chart is illustrated in Fig.5. The right-hand adjacent represents the instantaneous conductance, and the left-hand corner of equations represents IC of the P-V module. The variation ratio in output conductance is the same as the negative output conductance. The PV array will run at the MPP. Where V is PV voltage, I is PV current.
The most effective point is at MPP when the P-V curve slope is zero, and the voltage adjustment algorithm will stop as in the following equation**:**

$$\frac{dI_{PV}}{dV_{PV}} = -\frac{I_{PV}}{V_{PV}} \quad \text{At MPPT} \tag{2}$$

$$\frac{dI_{PV}}{dV_{PV}} > -\frac{I_{PV}}{V_{PV}} \quad \text{Left of MPPT} \tag{3}$$

$$\frac{dI_{PV}}{dV_{PV}} < -\frac{I_{PV}}{V_{PV}} \quad \text{Right of MPPT} \tag{4}$$

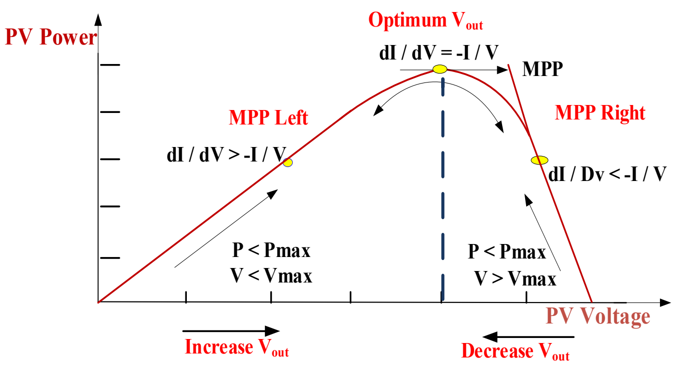

Figure 4. INC algorithm power - voltage curve.

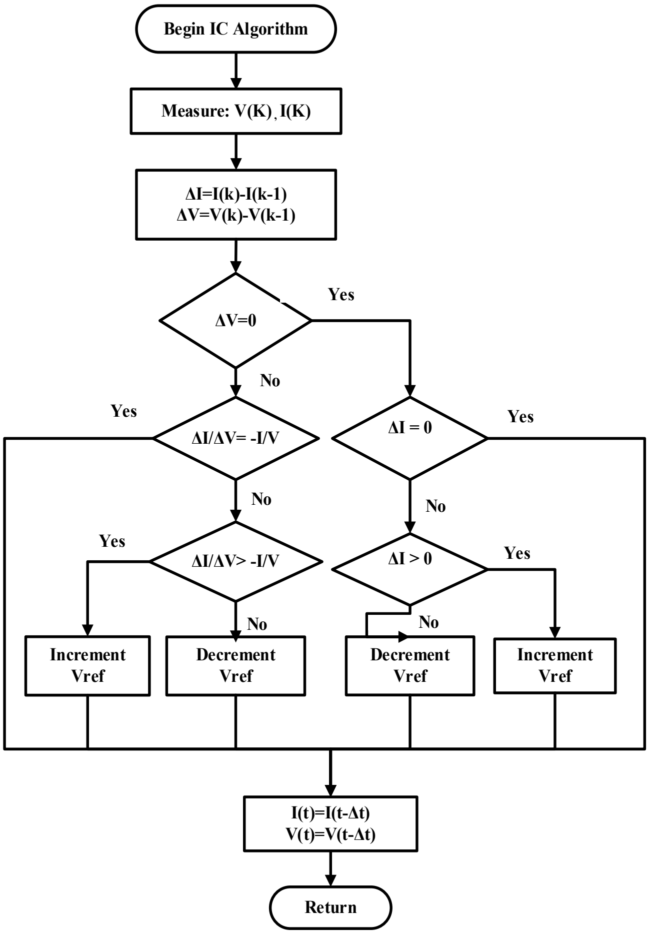

Figure 5. The INC algorithm flowchart.

B. Perturb & Observe method (P&O)

P&O technique was developed by examining the ramp (*dP/dV)* on the *P–V* qualities of the PV module. The ramp (*dP/dV)* > 0 at the left of MPP and (*dP/dV)* < 0 at the right of MPP. So, it is dependent on the ramp mark, to track the top power, the operating voltage must be perturbed. In previous literature, it has been indicated that P&O can be performed either by direct duty ratio control [31] or using a proportional-integral (PI) controller to control the voltage reference [30]. With tracking time and steady-state oscillations that depend on the size of the disturbance step, you can determine the tracking performance for P&O. The size of a smaller disturbance step produces fewer oscillations but at the same time produces a response.

On the other hand, the size of the big turbulence step increases the vibrations of the stable state [1,6 and 11]. After that, to improve the quality of P&O, a different perturbation step size is utilized in [1], [6], and [11]. Finally, the conventional P&O MPPT algorithm is upgraded based on the ramp *(dP/dV)* fluctuation on the *P–V* properties of the PV module. From the *P–V* properties as exposed in Fig. 6, it can be visualized that the ramp is positive at the left of MPP. Figure 6, .illustrates the photovoltaic output power versus the plate voltage at specific radiation. There are two locations to run as a point A (dP / dV > 0) and point B (dP / dV <0). When the small step size of the voltage is used, it reaches the small, steady-state oscillations with a slow MPPT response result and increases the power loss. At the bottom line, there are three constraints connected with the typical MPPT controller. The primary one is answerable for huge fluctuations around the MPPT. The next constraint is the controller short speediness reply. The third one can drop the MPP drive below fast varying radiation. The flowchart of the P&O MPPT algorithm is shown in Fig 7, and the sign of the ramp shows the negative on the right to track peak power. The duty cycle must be turbulent. The duty cycle is inversely proportional to the PV voltage i.e., Lower PV voltage leads to an increase in the working cycle and vice versa.

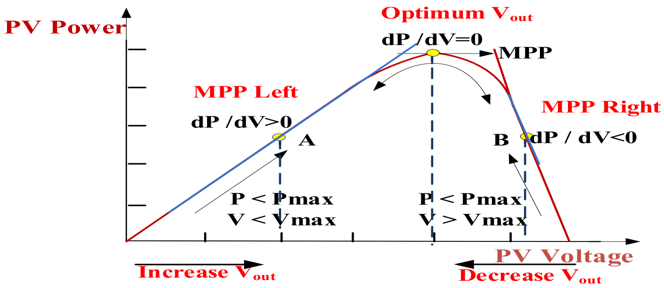

Figure 6. P&O three modes of operation.

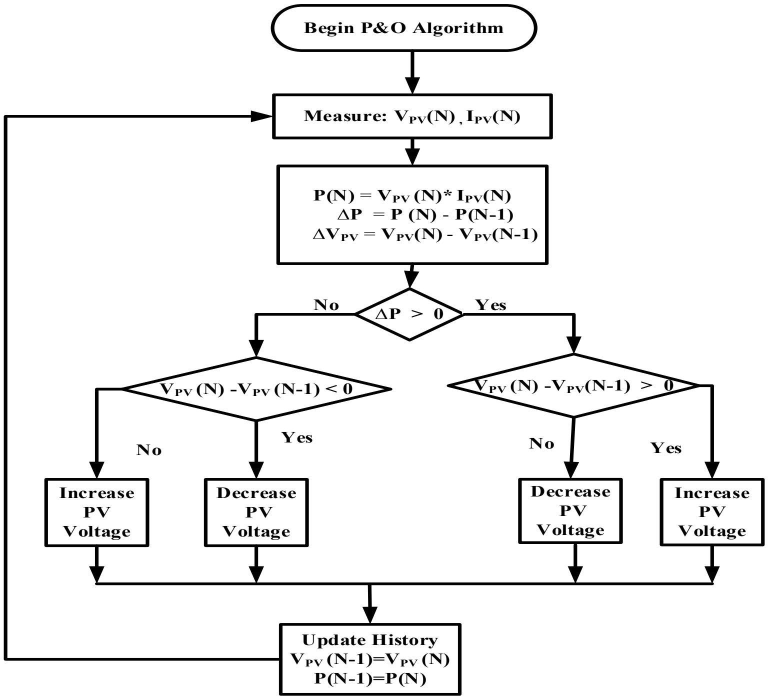

Figure 7. The P&O algorithm flowchart.

4. Voltage Ride-Through (VRT) System Molding

Figure 8 illustrates the system under study. It is indicated in some international regulations [19-23], that DG PV systems connected to the grid at a residential level to protect their interfacing inverter must be disconnected from the grid. In the requirements of this grid, prerequisites are imposed such as anti-islanding condition and power quality of the Grid - connected inverter. Though, the network requirements of DG systems are developed and adjusted based on the level of growth and penetration of the grid-connected DG PV systems due to the rapidly growing installations of the three-phase grid-connected PV systems. This model generates 250kw, and the connected distribution system is 20 kV as shown in Fig (8), it releases 110 kV of electricity into the grid. Figure (8) also illustrates the location of Simulink short circuit faults and sag faults applied to three distances of the PCC modeled on the 20 kV utility Grid. Future PV systems connected to the grid must fully support the public grid by riding through grid failures. These include wind power systems connected to medium and high voltage public grid known as LVRT capability.

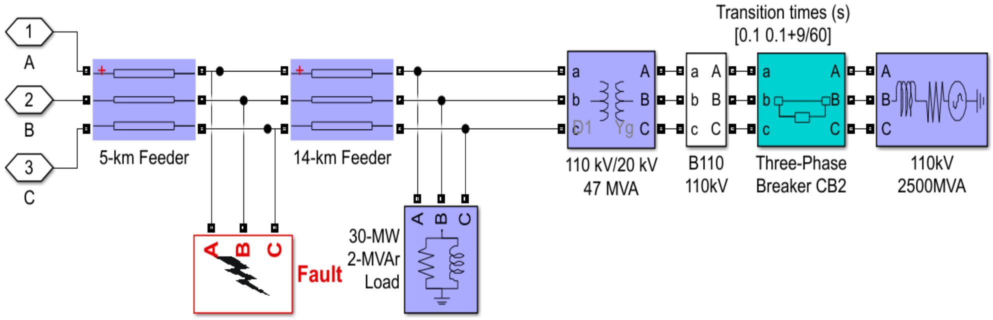

Figure 8. Schematic diagram of system under study.

A. Crowbar Strategy

Many papers have been done on different types of LVRT strategies, and in this paper, we're going to talk about the crowbar strategy. It is a circuit plugged into PV generators to protect it when there is a fault in the grid voltage. The traditionally used crowbar in the fault current path involves pure resistance [19-23]. Characterization of resistance belongs to the energy-dissipating element. When a fault occurs in the grid, the current will flow against the circuit resistance, the rest of the power will be consumed in the form of heat. This circuit also consists of two electronic power switches which operate based on a fault detection mechanism as shown in Fig.9. These keys cannot function together but only one key will operate at a time with or without a fault switching depending on the system condition, fault detection mechanism when an fault is immediately detected, is turned on (with fault switch) and turned off (without fault switch) and also includes current fault resistance.

These switches are used to signal AC to perform semi - positive and negative cycles, which are DIAC electronic switches.

5. Simulation Results and Discussion

The proposed system of grid-connected PV array is simulated at two types of MPPT (INC and P&O) and various types of faults that occur in the 20kV utility grid as is shown in Fig.8.At an ambient temperature of 25°C the simulations are running. The solar radiation was implemented employing the ramp profile. The solar radiation at 1000W/ m^2 begins, then gradually decreases to 250 W/ m2, then increases again until it reaches 1000W/ m2 as shown in figure 10. The model operating time is 0.8 seconds, and the faults are implemented in a time of 0.15 a second from 0.4 to 0.55.

The simulation results are presented starting from PCC, followed by the VSC inverter and boost converter and continuing with the PV array to analyze the photovoltaic system and determine the effects of the failures in the power grid as a function of the location where the fault occurs. The system under study details are specified in Table 1.

A. Comparison between INC and P&O MPPT

The response and the comparison of the INC and P&O method are discussed and presented graphically in the following items. By simulation implementing the two methods on the MATLAB model, it was found that the INC method is more accurate than the P&O method and we will show the comparison between the two methods. Still, we will mention the results of the INC method only because it is more accurate.

The simulation results on the output of the solar array is shown in Figure 11, so that Figure 11a show the PV output voltage of the solar array, which is approximately 273.5V of 1000 W/m^2 radiation and 252V at 250 W/m2 radiation. Figure 11b shows the output current on the solar panels, which is 910A, when the solar radiation is 1000 W/m2, and at the irradiance of 250 W/m2, it is approximately 210A, which based on what was presented in terms of voltage and current, PV power was summation. With P&O method as shown in Figure 11c, is 250kw at 1000 W/m^2 radiation and 20kw cycles at 250 W/m2 radiation. Table 2, shows the efficiency performance of two methods through the possibility of tracking the maximum capacity of solar cells.

Figure 12 shows that the duty cycle performance analysis at boost converter between the INC and P&O method is between 0.5 and 0.6.

Table 1. System parameters

Parameters	Values
Maximum power of PV module	305.2 W
Short circuit current of PV module	5.96 A
Open circuit voltage of PV module	64.2 V
Maximum current of PV module	5.58 A
Maximum voltage of PV module	54.7 V
Parallel strings of PV array	165
Series-connected modules per string	5
Boost converter inductance	5 mH
Boost converter resistance	0.005 Ω
Boost converter capacitance	100 µF
Frequency of converter switching	10 kHz
DC link voltage	500 V
Filter inductance	0.25 mH
Filter resistance	0.015 Ω
Voltage of grid	25 kV
Frequency of grid	60 Hz
Step up transformer	260V / 25 kV

Table 2. PV output power under different radiation

Solar Radiation (W/m^2)	PV Output power (KW)	
	P&O MPPT	INC MPPT
1000	250	245
250	20	20

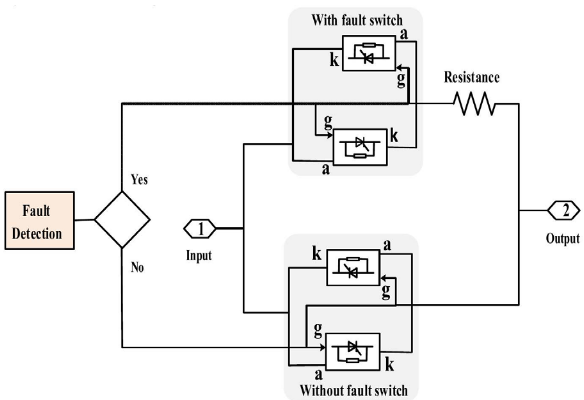

Figure 9. Schematic diagram of the Crowbar Scheme.

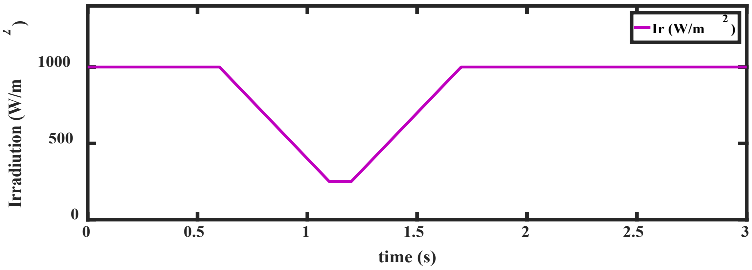

Figure 10. solar irradiution

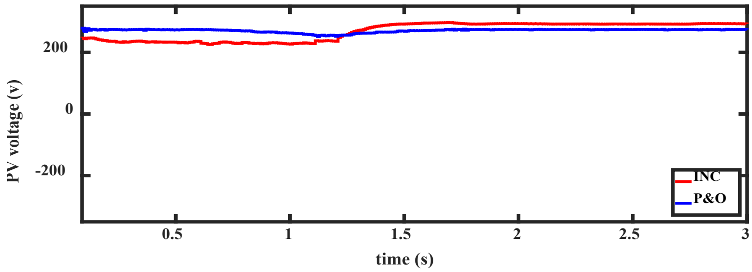

(a) PV voltage

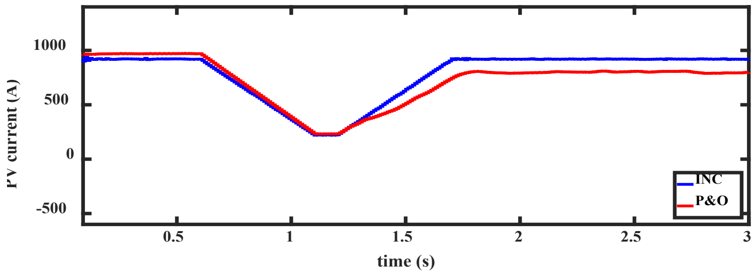

(b) PV current

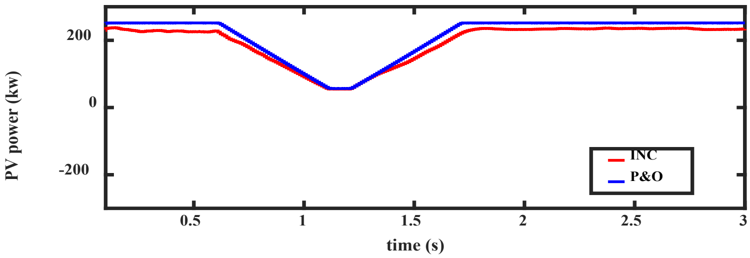

(c) PV power

Figure 11. The comparison performance analysis of PV system between INC and P&O method.

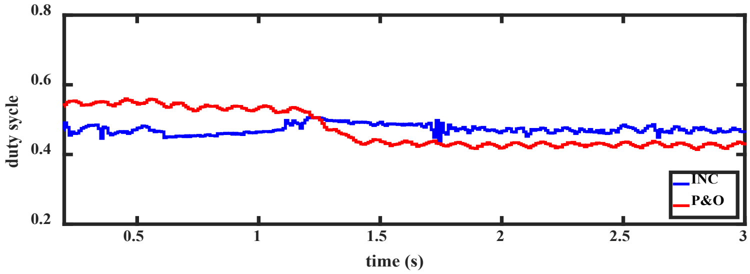

Figure 12. The duty cycle performance analysis at boost converter between INC and P&O method.

Figure 13 shows the voltage value of VSC, which is approximately equal in the two cases (INC & P&O) and is 500V

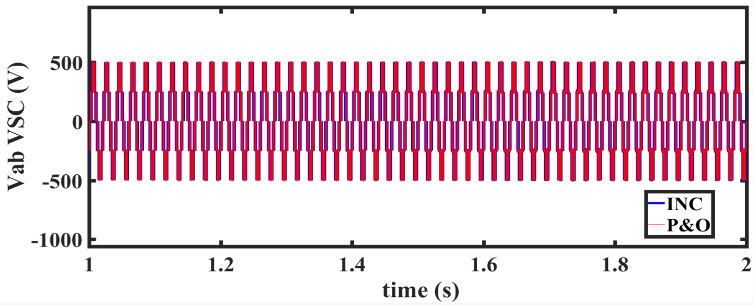

Figure 13. The inverter output voltage performance between INC and P&O method.

Figure 14 Show the grid power functioning of between INC and P&O method and note that the power value is 250kW at the radiation of 1000 W/m^2 and it is 60 kW at the radiation of 250 W/m^2.

Figure 15 shows the effective rms voltage for the three phases at 260 V, in which the voltage value is almost constant 260v V. Fig.16, shows the effective rms current for the three phases at 260 V, in which the voltage value is almost constant 260 V.but the current changes with the change of solar radiation where at 1000 W/m^2, the current is approximately 550A in both cases and begins to decline gradually as the solar radiation drops to 190A at 250 W/m^2

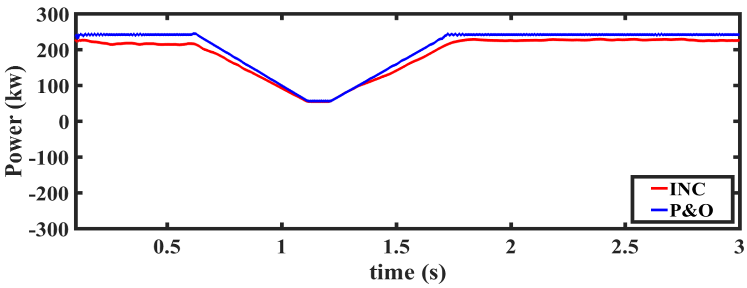

Figure 14. The grid power performance of between INC and P&O method.

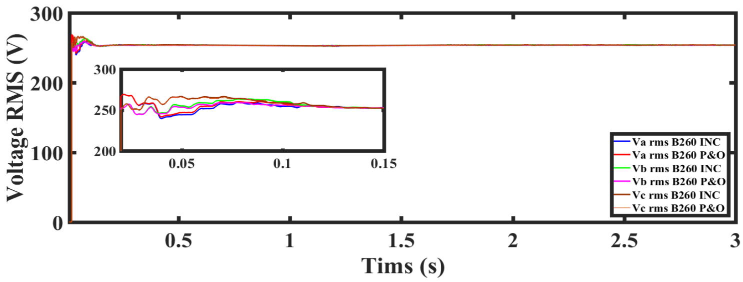

Figure 15. The inverter output (rms) voltage performance between INC and P&O method at 260v.

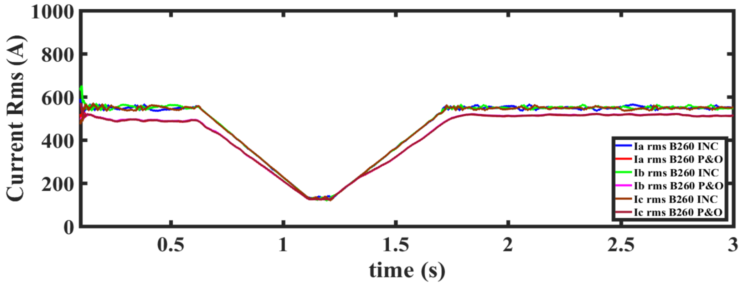

Figure 16. The inverter output (rms) current performance between INC and P&O method at 260v.

Figure 17, shows the grid voltage for the three phases at 20 kV, in which the voltage value is almost constant 20 kV. Fig.18, shows the grid current varies with the change of solar radiation. At 1000 W/m^2, the current is approximately 6.8 kA in both cases and begins to decline gradually as the solar radiation drops to 2.3 kA at 250 W/m^2.

Figure 19.a. The sine wave grid voltage performance between INC and P&O method at phase a. The grid voltage for phase a at 20 kV, in which the voltage value is almost constant 20 kV. Fig.19.b, shows the grid current varies with the change of solar radiation.

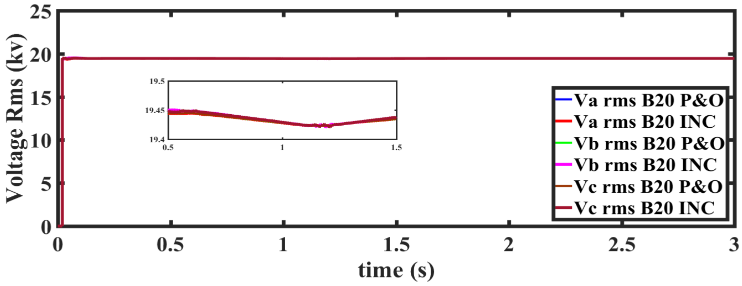

Figure 17. The grid voltage performance between INC and P&O method at 20 kv.

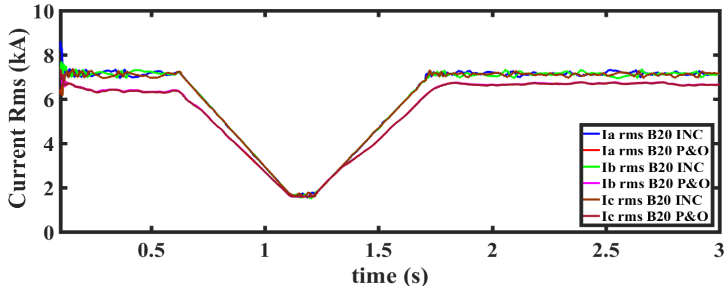

Figure 18. The grid current performance between INC and P&O method at 20 kV.

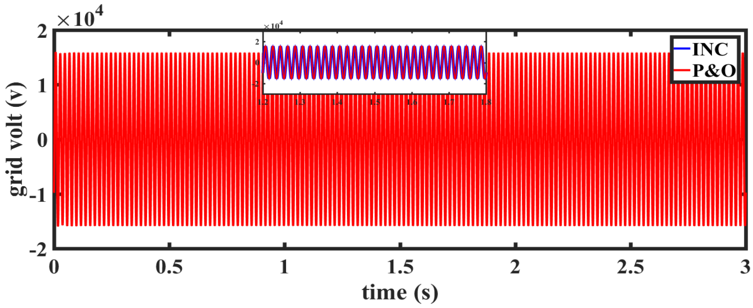

(a) Grid voltage at phase a

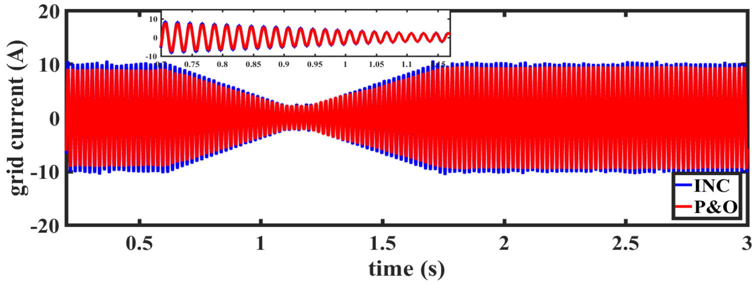

(b) Grid current at phase a

Figure 19. The AC grid voltage and current performance between INC and P&O method at phase a.

B. LVRT Results and Discussion

There is a slight difference between the types of short circuit &sag faults: the value of the fault resistance in the case of short circuits almost reaches zero. Therefore the value of the voltage is zero and the current is a very large value, but in the case of fault there is a value for the fault resistance and thus there is a value for the error voltage and current no be very large. The PV system during various types of short circuit grid faults as shown iv table 3

In the following part of this paper, the study of the different types of faults will be improved by the Crowbar strategy displayed at the beginning of this paper.

B.1. Single phase to ground short circuit fault

It is the most common and most frequent of all fault cases mentioned, although it appears to be a minor fault, but it is the most important case of fault. According to the Egyptian grid code, the model ran time is 0.8 seconds, and the fault time was set as 0.15 seconds. The fault time from 0.4 to 0.55 seconds, in all cases of fault, this time was determined. Then, the fault was performed on the model and corrected. Results are shown in Fig 20 and Table1, where output PV (voltage-current-power) in case of single phase to ground fault before and after the improvement.

Figure 20.a shows the value of the PV cell potential, which in fault condition is 271V to 277V but after optimization approaches is based on the crowbar scheme its normal value of 272.5V and the system normal value of 273V. The value of the PV current is shown in the fig 20.b and in fault ranges from 905A to 930.5A But after the optimization process approaches the normal current and is 911 and the normal value of the system is 910A. The power value of the cell is almost the same in the fault and after optimization; in fault the power is reduced to 249.5KW and after optimization to a natural value of 250kW, shown in fig 20.c. The value of DC voltage is finally shown in a fig 20.d. It ranges from 499.5V to 500.5V in case of fault, but after the optimization process it approaches a normal value of 500V The normal value until the system is stable and functioning is 500V.

Table 3. Simulation results of the PV system during various types of short circuit grid faults

Type of fault	Crowbar strategy	Dc-link voltage (V)	PV Array		
			Voltage (V)	Power (KW)	Current (A)
Normal operating conditions	Without	500V	273V	250KW	910A
Single phases fault to ground	Without	499.5-500.5V	273V	249.5KW	905-930.5A
	With	500V	271-277V	250KW	911A
Two phases fault	Without	450-700V	272.5V	199.5KW	990-1000A
	With	449.5V	80-290V	250KW	908-912A
Two phases to ground fault	Without	1050V	274.5V	180KW	924A
	With	500.5V	170-289V	250KW	909.5A
Three phases fault	Without	2800V	271.5V	87KW	0-998.5A
	With	498-502.5V	6V	246KW	901-914.5A
Three phases to ground fault	Without	2798V	269-275V	246KW	0-1000A
	With	496-503V	5V	240KW	896.5-912.5A

B.2. Two phases short circuit fault

Figure 21 and Table 1, shows the results of the output PV (voltage-current-power) in the case of two-phase fault before and after the improvement. Fig.21. a. shows that the PV voltage in the case of a fault is below the normal required voltage of about 273.5V to (80-290V), but after the optimization process it returns to normal voltage 274.5V. Fig.21. b, shows that the PV current in the case of a fault is below the normal required current of about 910A to range from 990A to 1000A, but after the optimization process it returns to normal current from 908A to 912A.

It is normal that in the event of a fault the grid voltage and current changes, resulting in the malfunction of the grid power. It can be shown in Fig.21.c, where the power of the grid in the case of a fault is 199KW, but after improvement it is returned to the normal power 250KW. The most important part where improvement should occur is DC voltage output of boost converter circuit, because it's the one that gives the DC voltage directly to the inverter. This value must be constant for the inverter to produce an exact output. The DC voltage shifts from the desired value of 500V to range from 450V to 700V in the case of fault, however, after optimization the desired value at which inverter operates is shown as 449.5V.

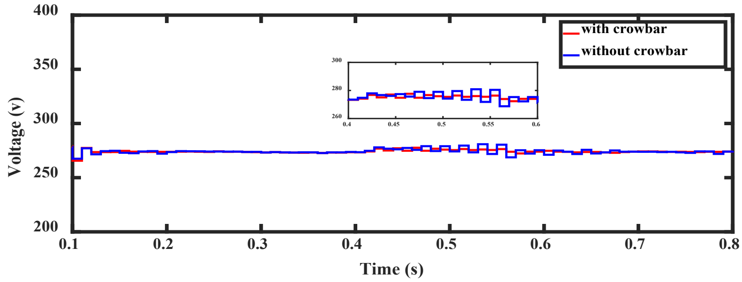

(a) PV voltage

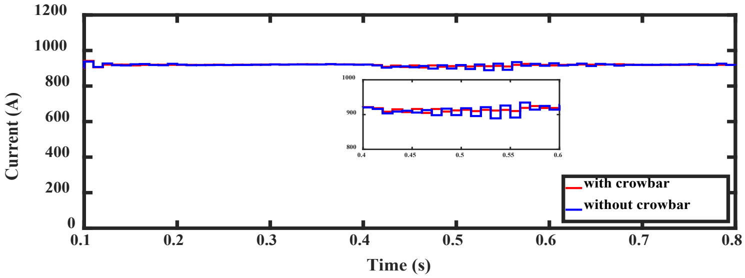

(b) PV current

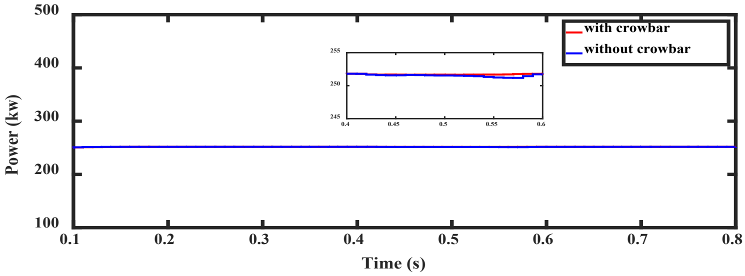

(c) PV power

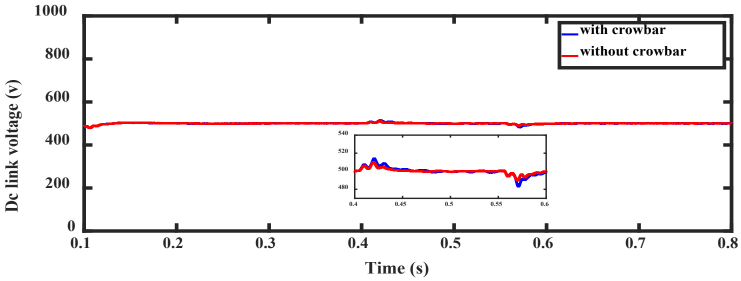

(d) Dc- link voltage

Figure 20. PV system response at grid single phase to ground fault.

B.3. Two phases to ground short circuit fault

Figure 22, and Table 1, shows the value of output PV (voltage-current-power) in the case of two phase to ground fault. These results appeared after operating using Crowbar strategy, which gave complete stability to the system. Figure 22a, showing the value of the PV voltage after optimization, which goes from (170-289V) to 271.5V and Figure 22b, showing the value of the PV current after optimization, which goes from 924A to 9095A. The voltage and current improvement resulted in a power improvement that went from 180KW before the improvement to 250KW after the improvement, as shown in the Figure 22c, the value of DC voltage is finally shown in a figure 22d. It ranges from 1050V to 500.5V in case of fault, but after the optimization process it approaches a normal value of 500V, the normal value until the system is stable and functioning is 500V.

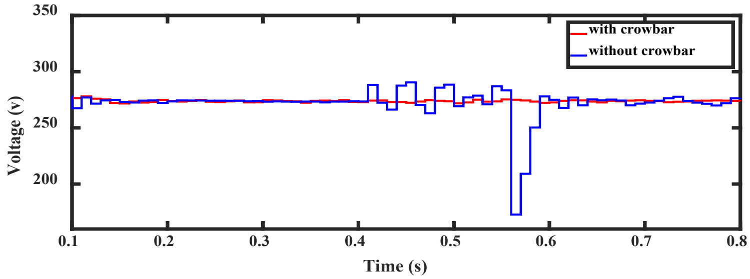

(a). PV voltage

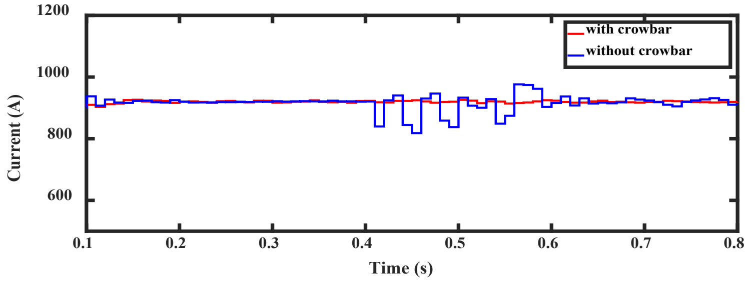

(b). PV current

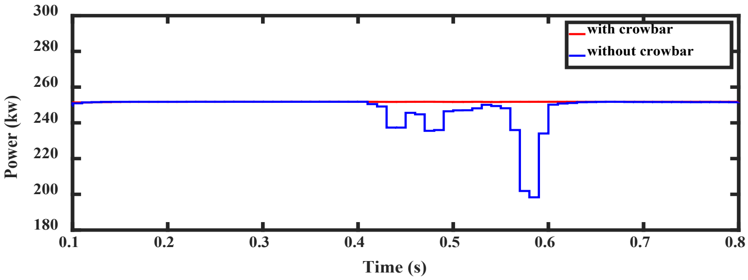

(c). PV power

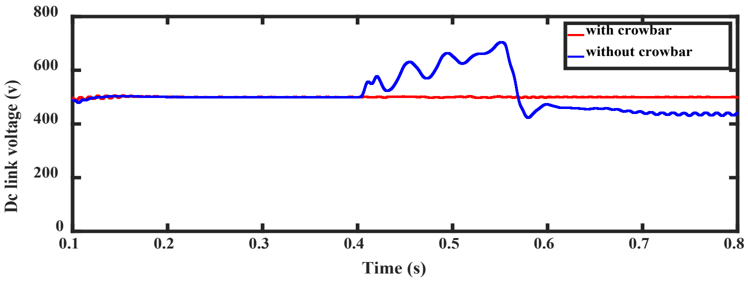

(d). Dc link voltage

Figure 21. PV system response at grid two phase short circuit fault.

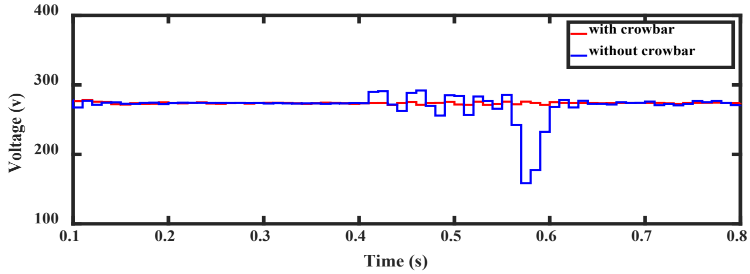

(a). PV voltage

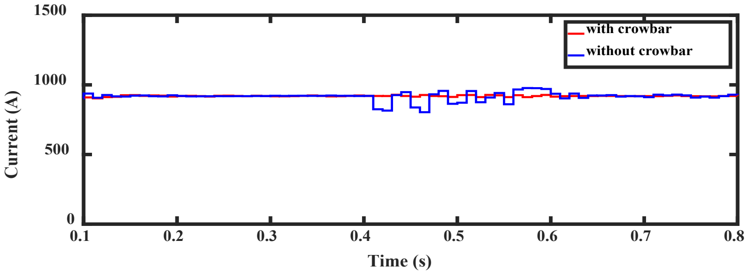

(b). PV current

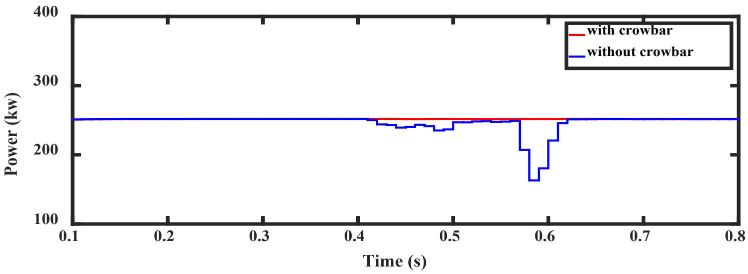

(c). PV power

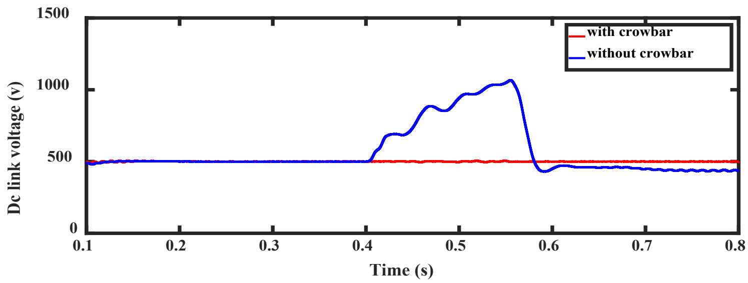

(d). Dc-link voltage

Figure 22. PV system response at grid double ground phase short circuit fault.

B.4. Three phases short circuit fault

Figure 23. and Table 1, shows the value of output PV (voltage-current-power) and also the value of Dc link voltage in the case of three phase fault, In this case, the fault is relatively greater than the previous cases, so the improvement is also less, but it works to operate the system in a stable state. In this case the voltage drops to approximately 6V before optimization as shown in Fig.23.a, but after the improvement process, it returns to its natural value, which ranges from

269V to 275V. Also, the current in case of a fault drops to (0-998A) as shown in fig.23.b, but after the improvement, it returns to (901-914.5A).

Figure 23c shows the power value before the optimization process is 87KW but after the optimization process it becomes 246KW. In the case of a fault, the value of Dc link voltage is very high, approaching 2,800V, as shown in Fig.23.d, but after the optimization, the voltage is (498-502.5V).

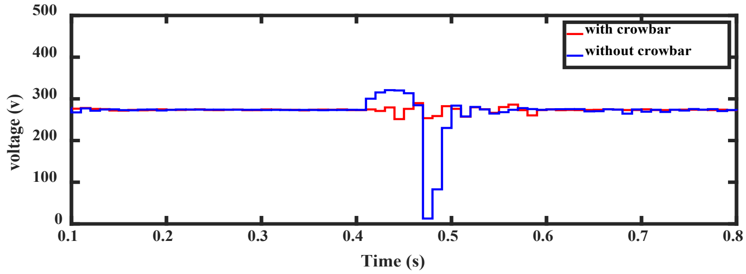

(a). PV voltage

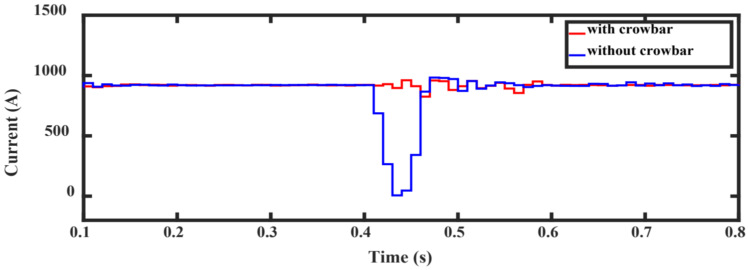

(b) PV current

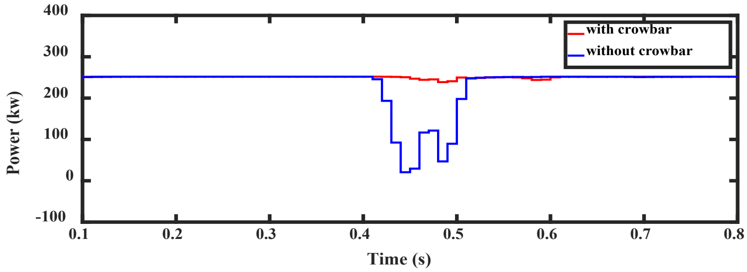

(c) PV power

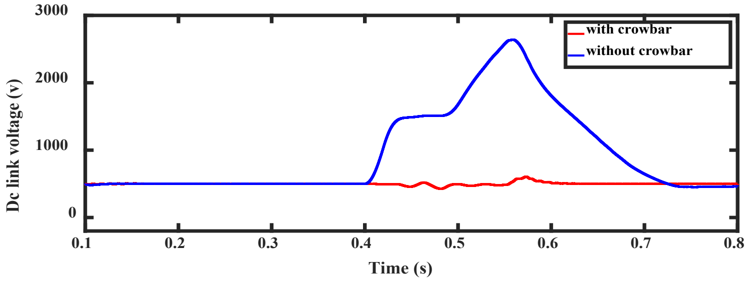

(d) DC voltage

Figure 23. PV system response at grid three phase short circuit fault.

B.5. Three phases to ground fault

Figuer 24, and Table 1, illustrates the value of output PV (voltage-current-power) in the case of three phase to ground fault. In this case, there is no significant difference from the previous case with a slight increase in the fault, but after using crowbar method, the system was operated in a stable state and this is evident through these results.

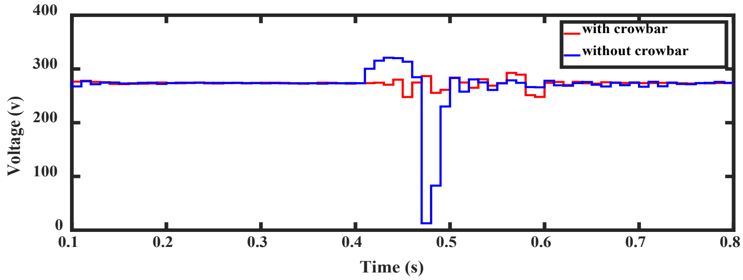

Pv voltage

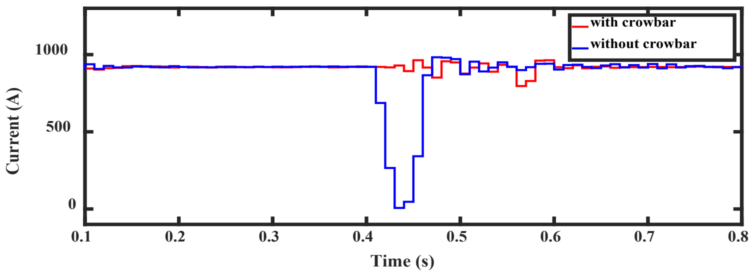

PV current

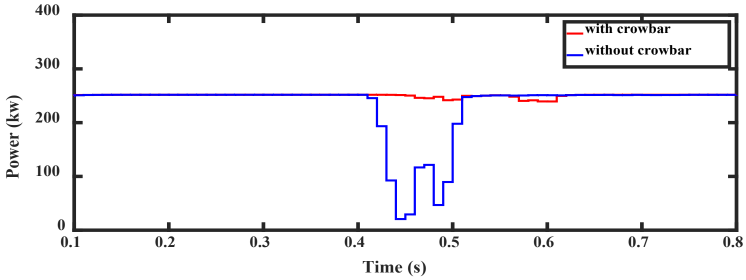

PV power

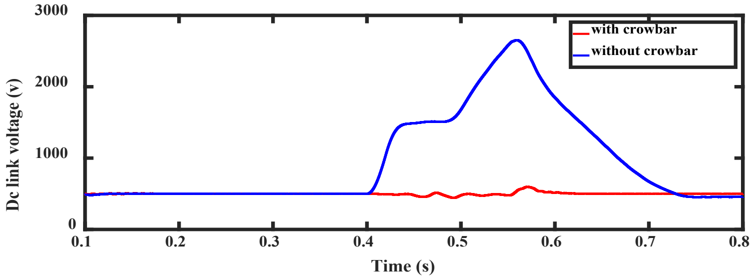

Dc link voltage

Figure 24. PV system response at grid three phase to ground fault.

6. Experimental work of grid connected PV system

Figure 25 illustrates the experimental setup of grid-connected photovoltaic systems, consisting of a PV power supply, three-phase transformer, three-phase DC to AC inverter and MPPT unit. The theoretical and experimental proposed system aims to study the performance and analysis of grid-connected photovoltaic systems under the influence of variable solar radiation.

The proposed system is composed of the following: A group of PV cells to produce electrical energy, DC / DC Boost Convert, A voltage DC link capacitor, the inverter for Converts the PV voltage into a variable voltage, the harmonic filter circuit RL and the transformer to raise an electrical voltage used to raise the voltage to suit the voltage of the public electrical grid. The data and description of the experimental system are presented in Table 4.

Figure 25. Experimental setup of PV system.

Table 4. Experimental setup specifications for the PV system

Names	Values
PV module	
Maximum PV power	1500 W
Rated current in A	7.2 – 11.7 A
Rated voltage in V	100 - 240 V
ON-grid inverter	
DC input voltage in V	250 – 1000V
DC MPP Voltage in V	300 – 800V
DC current	11 A
DC Short circuit current	13 – 20 A
AC voltage	3*230 V
Frequency	50-60 HZ
AC Max. Current	7 A
Max. Power	3200 W
Step up transformer	
Primary Voltage	400 V
Secondary Voltage	450 V
Nominal Power	1000 VA

A. PV measurements

Figure 26 shows and illustrates solar radiation change under the ramp profile. We observe in the form of solar radiation starting from 325 W/m2 and gradually rise to 675 W/m2 and then dome slightly and then the radiation gradually decreases Up to 260 W/m2, then stability slightly, then gradually increase to 470 W/m2 and then stability slightly.

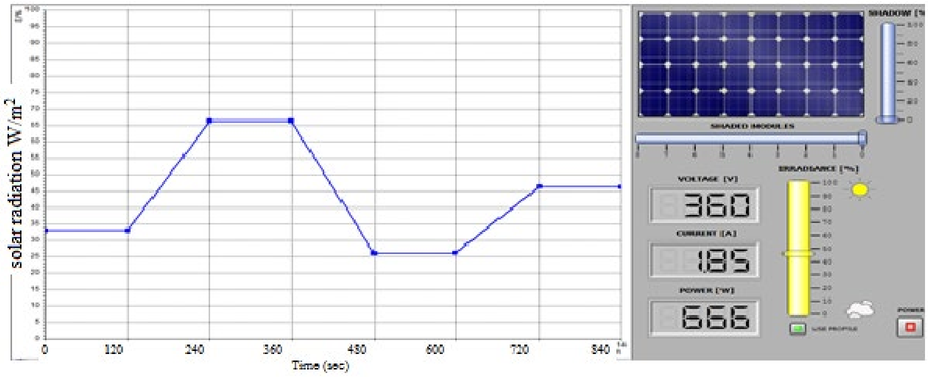

Figure 26. Ramp changes of solar radiation of experimental PV system.

Figure 27 shows the experimental performance of PV voltage, PV current, and PV power under the changes in the solar radiation ramp. As indicated in this Figure 27, (a) stable in the PV voltage from solar energy and Figure 27 (b) and (c) a change of PV power and PV current from solar energy with a change in the sun's radiation. The output power indicates the effectiveness of the MPPT system applied on the practical side.

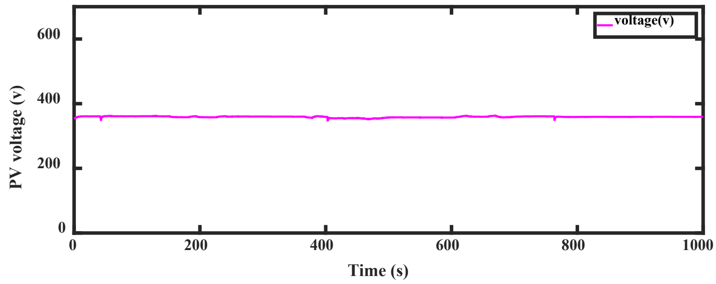

PV voltage

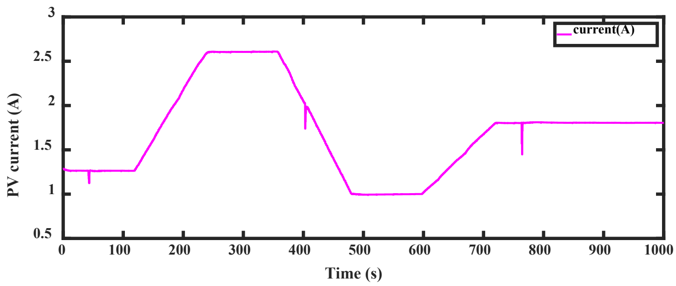

PV current

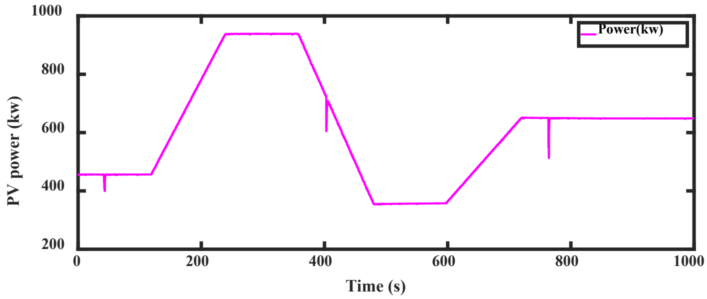

(c) PV power

Figure 27. Experimental performance of PV voltage, PV current and PV power.

B. Grid measurements

Figure 28 indicates the grid current value for phase (a) in the case of ramp changes of solar radiation. As shown in Figure 26, approximately the same value is proportional to the change in solar radiation.

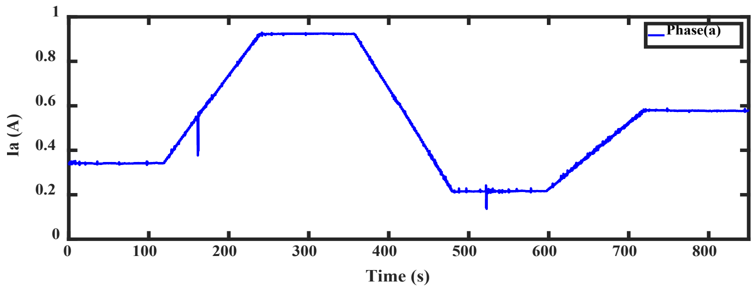

Figure 28. Experimental performance of grid current at phase a.

The grid voltage is fixed to the voltage required to connect under ramp changes of solar radiation. This is illustrated by Figure 29, which shows the grid voltage of phase (a) having almost constant values proportional to the change in solar radiation.

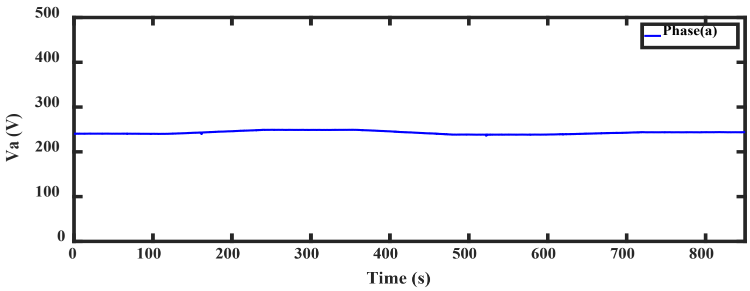

Figure 29. Experimental performance of grid voltage at phase a.

Figure 30, shows that the active and reactive power this figure shows that the active power increases with increasing solar radiation and decreases with decreasing solar radiation.

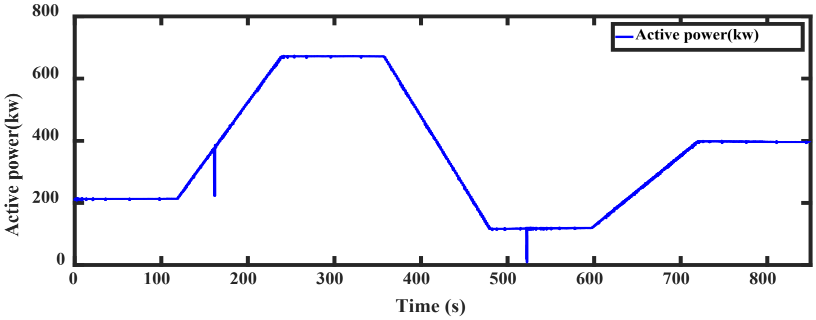

Active power

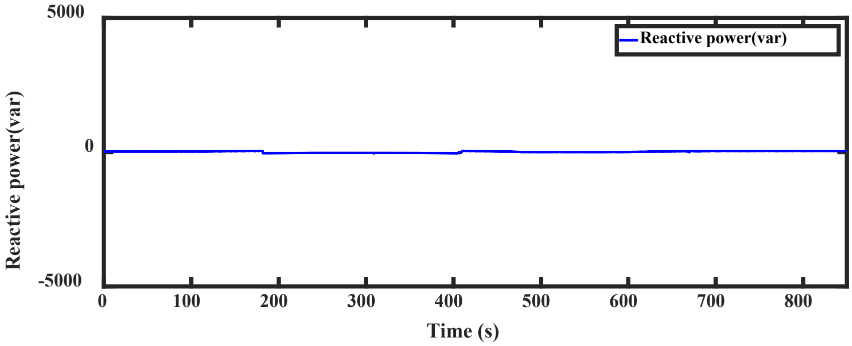

Reactive power

Figure 30. Experimental performance of grid active and reactive power

7. Conclusions

This paper introduces simulation in MATLAB / SIMULINK environment for grid-connected PV system. The main common failure that occur on the electrical grid is based on the different types of faults, and the effect of these failures on three-phase photovoltaic systems connected to the grid has been studied. This paper introduces theoretical verification of MPPT by P&O and IC technique and LVRT technology by crowbar technique. The grid fault events perturbed by the PV array, PV inverter, and PCC of the grid-connected PV system. The impact of grid faults on PV systems depends on the fault type and less on the fault distance. Symmetrical faults have a higher impact on PV systems performance than asymmetrical faults, both at the PCC and inside the grid-connected PV array. It also provides a comparison between two different types of different MPPT methods. The results of the solar system's power, current, and voltage output are displayed. The power, current, and voltage attached to the electrical grid were also shown. By comparing the P&O and IC method under various weather conditions, the IC was better for an average rate of maximum electric energy. In addition, based on the results, all the previous curves indicate a good compatibility in the overall results LVRT technology by crowbar technique**.** The results indicate good compatibility in the MPPT PV radiation between experimental results and simulation results.

8. References

[1]. S. A M. Abdelwahab, A. M. Hamada and W. S.E. Abdellatif “Comparative Analysis of the Modified Perturb & Observe with Different MPPT Techniques for PV Grid Connected Systems,” *International Journal of Renewable Energy Research-IJRER*, pp 156-164, vol 10, No 1, 2020.

[2]. Ahmed Elnozohy, Ali M. Yousef, Farag K. Abo-Elyousr1, Moayed Mohamed and Saad A M. Abdelwahab “Performance Improvement of the Hybrid Renewable Energy Sources

Connected to the Grid Using Artificial Neural Network and Sliding Mode Control," *Journal of Power Electronics*, Accepted, Feb 22, 2021.

[3]. A.M. Yousef, F.K. Abo-Elyousr, A. Elnozohy, M. Mohamed and Saad A. M. Abdelwahab, "Fractional Order PI Control in Hybrid Renewable Power Generation System to Three Phase Grid Connection", *International Journal on Electrical Engineering & Informatics*, vol 12, no 3, 2020.

[4]. S. A M. Abdelwahab, A. M. Yousef, M. Ebeed, F.K. Abo-Elyousr1, A. Elnozohy, M. Mohamed "Optimization of PID Controller for Hybrid Renewable Energy System Using Adaptive Sine Cosine Algorithm," *International Journal of Renewable Energy Research-IJRER*, pp 670-677, vol 10, no 2, 2020.

[5]. Elnozahy, A., Yousef, A.M., Ghoneim, S.S.M, S. A. M. Abdelwahab et al. Optimal Economic and Environmental Indices for Hybrid PV/Wind-Based Battery Storage System. *J. Electr. Eng. Technol*. Vol. 16, pp.2847–2862, 2021.

[6]. M. A. E. Eid, S. A. M. Abdelwahab, H. A. Ibrahim and A. H. K. Alaboudy, "Improving the Resiliency of a PV Standalone System Under Variable Solar Radiation and Load Profile," *2018 Twentieth International Middle East Power Systems Conference (MEPCON)*, Cairo, Egypt, pp. 570-576, 2018.

[7]. Saleh, B., Yousef, A.M., Ebeed, M. et al. Design of PID Controller with Grid Connected Hybrid Renewable Energy System Using Optimization Algorithms. *J. Electr. Eng. Technol*. Vol. 16, pp. 3219–3233, 2021.

[8]. S. S. Dessouky, A. A. Elbaset, A. H. K. Alaboudy, H. A. Ibrahim and S. A. M. Abdelwahab, "Performance improvement of A PV-powered induction-motor-driven water pumping system", 2016 *IEEE International Middle-East Power Systems Conference (MEPCON)*, Helwan University, Egypt, December 27-29, 2016.

[9]. S. A M. Abdelwahab, H. Y. Hegazy, W. I Mohamed. "Experimental investigation and theoretical for the performance improvement of MPPT technique with PV systems connected to the grid" *International Journal of Smart Grid and Clean Energy*, vol. 10, no. 4, October 2021.

[10]. M. A. E. Eid, A. A. Elbaset, H. A. Ibrahim and S. A. M. Abdelwahab, "Modelling, Simulation of MPPT Using Perturb and Observe and Incremental Conductance techniques For Stand-Alone PV Systems," *2019 21st International Middle East Power Systems Conference (MEPCON)*, Cairo, Egypt, pp. 429-434, 2019.

[11]. Adel A. Elbaset, Saad A. M. Abdelwahab, H. A. Ibrahim and Mohammed A. Elsayed Eid "Performance Analysis of Photovoltaic Systems with Energy Storage Systems," *Renewable and Green Energy, Springer*, January 2019.

[12]. S. S. Dessouky, S. A. M. Abdelwahab, W. S.E. Abdellatif and M. A. Ali, "Performance Enhancment of Grid Connected PV System by Using Incremental Conductance MPPT Technique," *Journal of Scientific and Engineering Research (JSERBR),* vol. 5, pp. 271-279, 2018.

[13]. Bahaa Saleh, Ali M. Yousef, Farag K. Abo-Elyousr, Moayed Mohamed, Saad A. Mohamed Abdelwahab & Ahmed Elnozahy, "Performance Analysis of Maximum Power Point Tracking for Two Techniques with Direct Control of Photovoltaic Grid -Connected Systems", *Energy Sources, Part A: Recovery, Utilization, and Environmental Effects*, 12 Mar 2021

[14]. W. S. E. Abdellatif, M. S. Mohamed, S. Barakat, and A. Brisha, "A Fuzzy Logic Controller Based MPPT Technique for Photovoltaic Generation System", *International Journal on Electrical Engineering and Informatics* – Vol. 13, No. 2, June 2021.

[15]. H. Shahida, M. Kamrana, Z. Mehmooda, M. Y. Saleemc, M. Mudassard, and K. Haider "Implementation of the novel temperature controller and ICMPPT algorithm for indoor photovoltaic system", *Solar Energy*, Vol. 163, pp.235–242, 2018.

[16]. M. M. Algazar, H. AL-monier, H. Abd EL-halim, and M. E. Salem, "Maximum power point tracking using fuzzy logic control", *Electrical Power Energy Systems*, Vol. 38, pp.21-28, 2012.

[17]. H. Chaouali, W. Ben Salem, D. Mezghani, A. Mami, "Fuzzy logic optimization of a centralized energy management strategy for a hybrid pv/pemfc system feeding a water pumping station", *International Journal of Renewable Energy Research (IJRER)*, Vol. 8, No. 4, pp. 2190-2198, 2018.
[18]. K. Amara et al., "Improved Performance of a PV Solar Panel with Adaptive Neuro Fuzzy Inference System ANFIS based MPPT," 2018 7th *International Conference on Renewable Energy Research and Applications (ICRERA)*, Paris, pp. 1098-110, 2018.
[19]. Islam, S.U.; Zeb, K.; Din, W.U," A Novel Design of FRT Strategy and Proportional Resonant Controller for Three Phase Grid connected PV System"*IEEE International Conference on Power Generation Systems and Renewable Energy Technologies,* pp 1-6, 2018.
[20]. M. J. Morshed and A. Fekih, "A Novel Fault Ride Through Scheme for Hybrid Wind/PV Power Generation Systems," in *IEEE Transactions on Sustainable Energy*, vol. 11, no. 4, pp. 2427-2436, Oct. 2020.
[21]. E. Buraimoh and I. E. Davidson, "Overview of Fault Ride-Through Requirements for Photovoltaic Grid Integration, Design and Grid Code Compliance," *2020 9th International Conference on Renewable Energy Research and Application (ICRERA)*, pp. 332-336, 2020.
[22]. M. N. Musarrat and A. Fekih, "A Fault Tolerant Control Framework for DFIG-Based Wind Energy Conversion Systems in a Hybrid Wind/PV Microgrid," in *IEEE Journal of Emerging and Selected Topics in Power Electronics*, 29 October 2020.
[23]. L. Min, X. Zhen and X. Jing, "Control Strategy of Doubly-Fed Induction Generators Based on Stator Virtual Impedance in Microgrid," *2020 39th Chinese Control Conference (CCC)*, 2020, pp. 5299-5304.

Saad A. Mohamed Abdelwahab received his B.S. and M.S. degrees from the Faculty of Technology and Education, Suez Canal University, Suez, Egypt, in 2006 and 2011, respectively. He received his Ph.D. degree from the Faculty of Technology and Education, Electrical Department, Suez University, Suez, Egypt, in 2016. **Dr. Saad A. Mohamed Abdelwahab** Associate Professor, Electrical Department, Faculty of Technology and Education Suez University in 2021. His current research interests include renewable energy sources, power electronics, power system optimization, high voltage systems, and power quality.

Adel A Elbaset was born in Nag Hamadi, Qena - Egypt, on Oct. 24. 1971. He received the B. S., M.Sc., and Ph. D. from Faulty of Eng., Electrical Eng. Dept., Minia University, Egypt, in 1995, 2000, and 2006, respectively. **Dr. A. Elbaset** is currently full Professor, Faculty of Eng., Heliopolis University works as a Vice-Dean for student affairs and Head of the Dept. Electromechanics. His research interests are in the area of Wind energy system, Photovoltaic, renewable energy system, power electronics, power system protection and control, power Quality and Harmonics, application of neural network and fuzzy system. Dr. Adel have 12 international Book in the field of Renewable energy.

Fahd Yousef received his B.S. degree from the Faculty of Technology and Education, Sohag University, Sohag, Egypt, in 2016; and his research interests is in the area of Renewable energy sources.

Walid S.E. Abdellatif was born in Kafr-Elsheikh, Egypt. He received the B.Sc. Degree in Industrial Education from the Suez Canal University, Suez, Egypt, in 2006. He received the Master of Industrial Education degree in Electrical Power & Machines from Suez Canal University, Suez, Egypt, in 2012, and Ph.D. from Faculty of Industrial Education, Electrical Department, Suez University, Egypt, in 2016. He is an Assistant Professor in Electricity Department (Electrical Power & Machines), Faculty of Technology and Education, Suez University, Suez, Egypt form 2016. His research interestsinclude renewable energy sources especially the wind energy issues, power electronics, micro grid and power quality.